JOURNAL OF GEOPHYSICAL RESEARCH: SPACE PHYSICS, VOL. 118, 832–838, doi:10.1002/jgra.50152, 2013

Ordering of injection events within Saturnian SLS longitude and local time

T. J. Kennelly,[1] J. S. Leisner,[1] G. B. Hospodarsky,[1] and D. A. Gurnett[1]

Received 18 October 2012; revised 22 January 2013; accepted 25 January 2013; published 28 February 2013.

[1] Periodicities similar to the Saturn kilometric radio (SKR) emissions have been observed throughout the magnetosphere in both the magnetic field and the plasma. An outstanding question is what mechanism links these periodicities between the inner and outer magnetospheres. It had been postulated that the interchange instability, where narrow injections return the magnetic flux carried by the bulk plasma outflow, could play a role in determining the periodicities, but early analysis found no ordering of the injection events in the SKR-derived Saturnian longitude system (SLS). In this study, we reexamine this possibility by limiting our data set to the young injection events observed by the Cassini radio and plasma wave science instrument. We find that the young injection events observed near midnight local time are strongly ordered by SLS. Further, this ordering varies with the Saturnian season. Pre-equinox, the northern hemisphere's longitude system controls the event occurrence. Post-equinox, the events are ordered by the southern hemisphere-derived longitude system. We suggest that this may be an effect in the variations in ionospheric conductivity or due to change in the magnetosphere's orientation relative to the solar wind.

Citation: Kennelly, T. J., J. S. Leisner, G. B. Hospodarsky, and D. A. Gurnett (2013), Ordering of injection events within Saturnian SLS longitude and local time, *J. Geophys. Res. Space Physics*, *118*, 832–838, doi:10.1002/jgra.50152.

1. Introduction

[2] Centrifugal interchange instability is important for transporting plasma radially in rapidly rotating magnetospheres, where colder, more dense plasma moves outward while hotter, less dense plasma is injected inward [*Hill*, 1976; *Siscoe and Summers*, 1981]. These plasma injection events are observed across different energies and scale sizes. High-energy, large-scale injection events have been observed at Jupiter with the Galileo spacecraft [*Mauk et al.*, 1997, 1999] and at Saturn, where the event scale size is >1 Saturn radii (R_S; 1 R_S = 60,268 km), with the Cassini spacecraft [*Mauk et al.*, 2005]. During most orbits when Cassini is in the inner magnetosphere, low-energy, small-scale (<<1 R_S) injection events are observed by the Cassini plasma spectrometer (CAPS) [*Young et al.*, 2005] and the Cassini magnetospheric imaging instrument (MIMI) [*Krimigis et al.*, 2005]. These events are characterized on energy-time spectrograms by dispersion in both the electrons and ions, but on opposite sides of the event, they are centered on magnetic perturbations [*Hill et al.*, 2005; *Burch et al.*, 2005; *Mauk et al.*, 2005].

[3] Previous studies have attempted to determine what modulates the creation of these small-scale injection events. *Chen and Hill* [2008] conducted a statistical analysis of the injection event distribution by analyzing CAPS data of Cassini's first 26 orbits. In the CAPS data, the dispersion of young events is observed but is often indistinguishable from "spikes" with a steep vertical slope [*Hill et al.*, 2005]. As a result of this, the young events (<1 h old) were excluded by the selection criteria.

[4] To estimate the location of the injection event creation, *Chen and Hill* [2008] used the calculated ages and the azimuthal velocity profile of *Wilson et al.* [2008] to work backward from the point of observation. This method requires the assumption that injection events corotate with the surrounding plasma. The resulting event creation locations were found to be ordered in local time (LT) (near dawn and dusk) and L shell, but not in the Saturn longitude system (SLS). The Saturn longitude system used in this study was SLS 3 [*Kurth et al.*, 2007; 2008], a previous longitude system valid from January 2004 to August 2007. Large-scale injection events have also been found to be ordered in local time, preferring the midnight-to-dawn sector, and were calculated to be much older than the small-scale injections in the CAPS observations [*Mitchell et al.*, 2009; *Müller et al.*, 2010].

[5] *Menietti et al.* [2008] analyzed a single injection event observed in October 2005 and found that the inward motion of the flux tube, and the related processes, created a non-Maxwellian electron distribution that was relatively depleted at lower energies (<107 eV) and enhanced at higher energies. The resulting gradients were able to generate the observed plasma waves, except for the electron cyclotron harmonics. Those emissions were postulated to have been

[1]University of Iowa, Iowa City, Iowa, USA.

Corresponding author: George B. Hospodarsky, University of Iowa, Iowa City, IA, USA (george-hospodarsky@uiowa.edu)

2169-9380/13/10.1002/jgra.50152

generated by a loss cone unseen by CAPS due to its orientation relative to the magnetic field. *Rymer et al.* [2009] observed that the *Menietti et al.* [2008] event was not typical of the injection events included in the previous CAPS studies. That event was estimated to be 15 min old, which is young when compared with the ages derived by *Chen and Hill* [2008]. These young injection events also have a strong signature in the radio and plasma wave science (RPWS) data [*Menietti et al.*, 2008; *Rymer et al.*, 2009; *Gurnett et al.*, 2004].

[6] Although young injection events appear in the RPWS data set as the occurrence or modulation of multiple, well-understood plasma waves including the upper hybrid emission [*Persoon et al.*, 2005], electron cyclotron harmonics [*Menietti et al.*, 2008; *Tao et al.*, 2010; *Gurnett et al.*, 2005], and whistler mode emissions [*Hospodarsky et al.*, 2008], they have yet to be used to study the interchange instability at Saturn. In this paper, we conduct such an analysis using all *Rymer et al.* -type plasma wave events observed from July 2004 through December 2011. This analysis not only examines occurrence in L shell and local time, but also uses the most recent SKR-derived longitude systems [*Gurnett et al.*, 2011] to examine whether the inward half of this plasma convection might have any role in communicating periodicities between the inner and outer magnetospheres.

2. Observations

[7] Selection of events was based primarily upon the presence of a strong background upper hybrid emission and a local lowering of the emission frequency caused by density decrease within the inward moving flux tube. When identified, each event was assigned a quality flag determined by the strength of the upper hybrid and the presence of the secondary plasma waves and/or magnetic perturbations. The presence of magnetic perturbations is interpreted from perturbations in the electron cyclotron frequency. Since our selection criteria require a strong background upper hybrid, our event observations occur primarily near the magnetic equator. In that region, the magnetic perturbations are predominantly field enhancements, as the field depressions occur at higher latitudes [*Leisner et al.*, 2005; *André et al.*, 2007]. About half of the events detected contained all of the secondary plasma waves at strengths significantly (>10 dB) above the background noise level, and the rest contained either some or none of the secondary signatures.

[8] Figure 1a shows an example of a high-quality event: there is a well-defined upper hybrid emission throughout the spectrogram, but there is also a clear decrease (in frequency) from 9:19 to 9:28. The enhanced cyclotron harmonics (3×10^3 to 1.7×10^4 Hz), magnetic field perturbation (the fluctuations in the electron cyclotron frequency (white line)), and whistler mode emissions ($\sim 10^3$ Hz) are also prominent during the event. For comparison, Figure 1b shows an event (~12:36 to 12:38) assigned a low-quality flag. The upper hybrid emission disappears, so it is unclear if its frequency decreased relative to the background, but there are some secondary signatures (small magnetic field perturbation and electron cyclotron emission) that suggest that this may be an injection event.

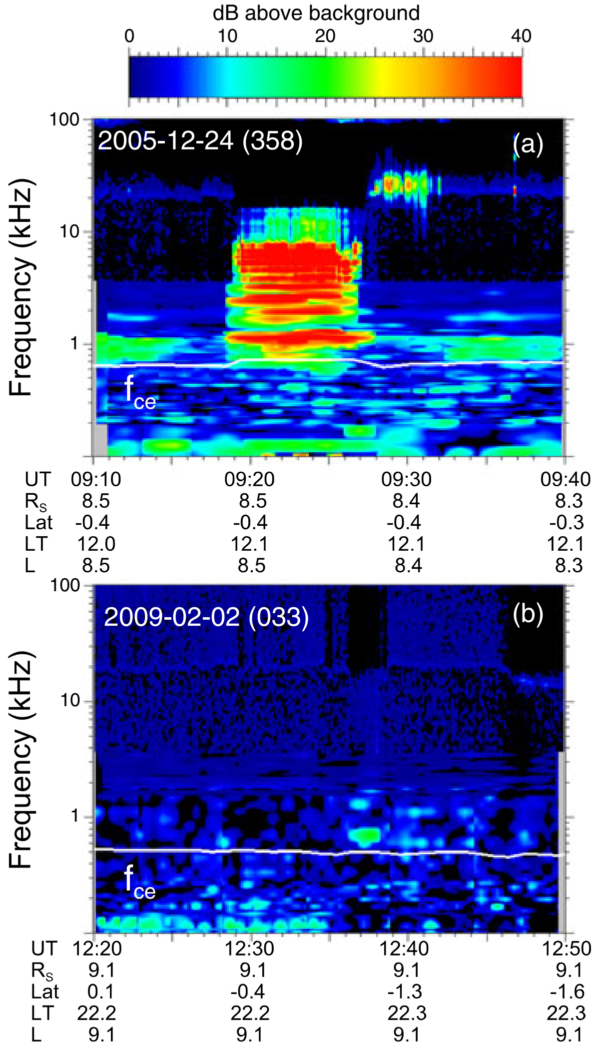

Figure 1. (a) An example of a high-quality young injection event at 9:19–9:28. This event is included in this study because of the well-defined upper hybrid emission with a clear dropout during the event, the enhanced cyclotron harmonics, and a magnetic perturbation. (b) An example of a low-quality young injection event at 12:36–12:39. This event was not included in this study despite the electron cyclotron emission and magnetic perturbations because of the uncertainty in the lowering of the upper hybrid emission due to the lack of a signal.

[9] Although the quality flag discriminates between the most certain and the less certain events, it is not able to counter observational biases. As *Persoon et al.* [2005] noted, the upper hybrid emission is strong and consistently present near the equatorial plane but less commonly observed away from it. In addition, both the upper hybrid and the injection events are restricted to the inner and middle magnetospheres [*Hill et al.*, 2005]. To prevent biases in data selection and normalization, this study is restricted to low-inclination orbits when the spacecraft was inside an L shell of 12 and within 2 R_S of the equatorial plane. High-inclination orbits were excluded completely due to the small amount of time spent in the near-equatorial region. After applying these restrictions, we found 422 events. Of those, 249 were assigned a high-quality flag and used in this study.

3. Analysis

3.1. Selection and Characterization

[10] Since the injection events are small structures (as seen in the RPWS data), the occurrence time recorded for each flux tube was the time at the center of the observation. Cassini's location at this central time was used for all positional analyses. We note that the SKR-derived SLS 4 longitudes, which we will refer to as North and South longitudes, were interpolated using 10 min resolution data from the University of Iowa's Cassini SLS 4 tool (J.B. Groene, http://cassini.physics.uiowa.edu/sls4/). In this system, the South longitudes are valid from 12 September 2004 to 9 January 2011 and the North longitudes are valid from 5 April 2006 to 16 September 2009 [*Gurnett et al.*, 2011]. With these date restrictions, there are 45 events that both have a North and a South longitude and 127 that only have a South longitude. The remaining 77 events were excluded from the analysis completely as they fell outside of these dates.

[11] In the previous section, we discussed observational biases that required restrictions on the data used. In our analysis, there are potential biases due to tour design that cannot be accounted for by this method. The first is in spatial distribution of observations: Cassini's orbital coverage of the Saturnian magnetosphere is not uniform for any of the spatial parameters examined. Different phases of the mission covered specific L shell and local time ranges, and similar orbits lead to a correlation between those two parameters. The other bias is in the injection events themselves. When an injection event is observed, it is common to see others nearby. This may represent a single location launching multiple flux tubes planetward in rapid succession, or it may represent a single flux tube that broke up [*Russell et al.*, 2005].

[12] We chose to account for these biases in the binning process. We can compensate for this by examining the occurrence rate, instead of just the occurrence number, of injection events as a function of position and by filtering out nearby events (see Appendix A for a discussion of these calculations). To allow for effects in the coupling between L shell and local time on certain orbit groups, we perform these rate calculations in a two-dimensional histogram.

3.2. Local Time and L Shell

[13] The young injection events are detected by RPWS between 4 and 11 R_S, although they are rarely observed at the ends of this range (Figure 2). The occurrence with L shell is nearly identical to that found by *Chen and Hill* [2008]. The small differences between the two profiles are most likely due to *Chen and Hill* being sensitive to older

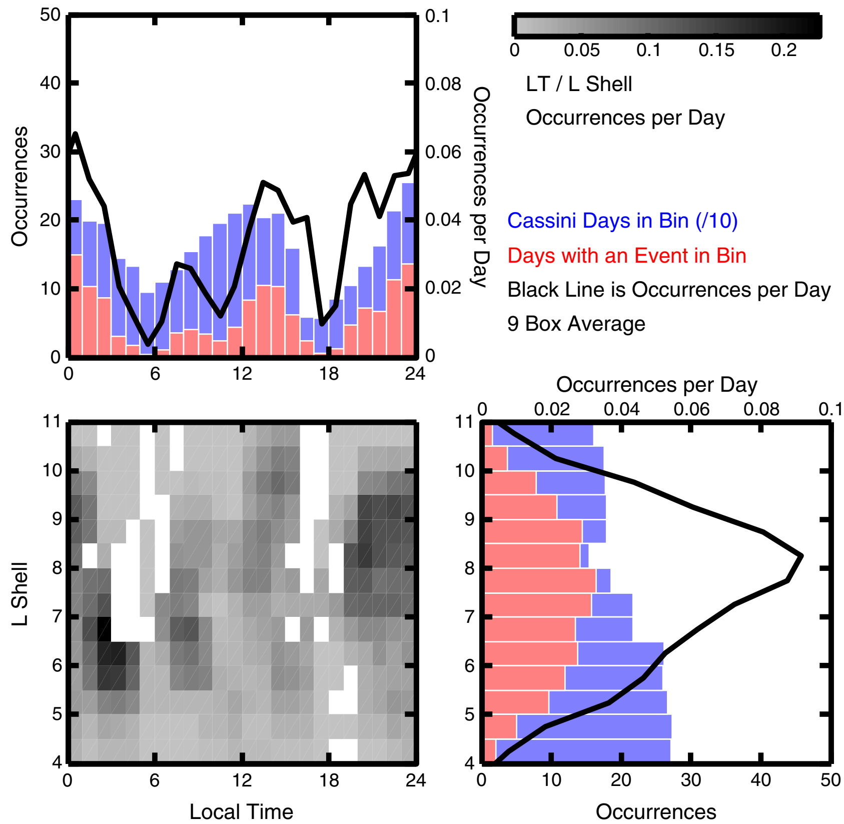

Figure 2. Occurrence of injection events in local time and L shell. Events are binned in (bottom left) a two-dimensional histogram according to their L shell and local time values which is then summed across the *x* and *y* axis to produce (bottom right) the L shell and (top left) local time distributions, respectively. The bin sizes are 1 h and 0.5 L shell. The days Cassini visited each bin are represented by blue bars and are divided by 10 for visibility. The red bars represent the number of injection events observed in that bin. There are 141 events in total. The heights of the blue and red bars represent number of occurrences and the color of the two-dimensional histogram and the black lines on the standard histograms represent occurrences per day.

flux tubes, increasing the number of observations at the ends of the range.

[14] In local time, we find that the largest occurrence rates are in the near-midnight (19–3 LT) and post-noon (11–17 LT) sectors. As shown by the blue bars, Cassini spent less time in the local time ranges where we found few events, but with over 50 passes through each, the effect on the occurrence rate should be small. Unlike the L shell variation, our local time profile is very different from that calculated by *Chen and Hill* [2008].

[15] Using the background plasma velocity, *Chen and Hill* [2008] traced the flux tubes back to the local time of their creation and found a bimodal distribution centered on local times of 8 and 19. Figure 2 shows that we also find a bimodal distribution, but it is one where the events are clustered around midnight and in the post-noon sector. The shift between these two profiles is about 4 h of local time. This difference may be explainable if the flux tubes are moving significantly faster than the background flow, as published by *Wilson et al.* [2008].

3.3. SLS 4 Longitude

[16] When all events were analyzed together, we found no control of their occurrence by either SLS 4 North or South. There is, of course, no a priori reason to assume that all injections in all parts of the magnetosphere through the entire Cassini mission would be generated in a single longitude sector. *Mitchell et al.* [2009] found that large-scale injections recur in the midnight-to-dawn sector and are well correlated with SKR. In the post-noon sector, *Radioti et al.* [2009] observed transient structures in the post-noon sector of Saturn's aurora that were correlated with large-scale injection events observed concurrently at low-to-middle latitudes. Given this studies' separation of these local times and the apparent separation in our event occurrences (Figure 2), we use this division for our analysis. Table 1 shows the number of events in each sector for North and South's time ranges.

[17] Cassini spent little time in the post-noon (11–17 LT) sector during the period when North is valid (April 2006 to September 2009), so we are unable to search for any ordering in that longitude system. For South, there were 41 events that appeared evenly distributed across all longitudes. The near-midnight region (19–3 LT) contained more events for both longitude systems: 72 in South's time range and 20 in North's. In North, the events all occurred in a hemisphere centered near 160°. In South, the events were evenly distributed except for a minor peak near 120°.

Table 1. Binned Event Counts in SLS 4 Longitude Divisions

	SLS 4 North[d]	SLS 4 South[e]
Post noon [a]		
Pre-equinox	1	17
Post-equinox	N/A	24
Near midnight [b]		
Pre-equinox	20	50
Post-equinox	N/A	22
Total [c]	31	121

[a]Post noon includes events from 11–17 local time.
[b]Near midnight includes events 19–3 local time.
[c]Includes post noon, near midnight, and events that lie outside of these times.
[d]SLS 4 North is defined from 5 April 2006 to 16 September 2009 [*Gurnett et al.*, 2011].
[e]SLS 4 South is defined from 12 September 2004 to 9 January 2011 [*Gurnett et al.*, 2011].

[18] As previously mentioned, there is a time issue in this analysis. The period of validity for South (September 2004 to January 2011) includes pre-equinox and post-equinox times (equinox was in August 2009). At equinox, the subsolar point moved from Saturn's southern hemisphere into the northern hemisphere. Since Saturn's magnetic and rotational axes are aligned, this seasonal change switched the magnetospheric hemisphere exposed to solar wind flow. This also changed which pole received more solar illumination, which affects the ionosphere's Pedersen conductivity [*Gurnett et al.*, 2009]. The interchange instability growth is suppressed by high ionospheric conductivity, so injection events may reflect conductivity variations in the darker polar region [*Southwood and Kivelson*, 1989]. Saturn's offset magnetic dipole [*Dougherty et al.*, 2005] does not shift this conductivity dominance until after equinox, but we neglect that effect here.

[19] When the post-noon events are separated at equinox, no new structure appears. For the near-midnight events, the lack of post-equinox events for North does not change the previous description of that ordering (Figure 3a). When the near-midnight events defined for South are separated at equinox, however, the distribution does change. Pre-equinox, the events are nearly evenly distributed in South (Figure 3b). The injections that formed the "minor peak" in South occurred post-equinox (Figure 3c), where they are now unobscured by the pre-equinox distribution.

[20] Our estimate for longitudinal control uses the probability (0 to 1) that the observed (or higher) concentration of events in a longitude range could have occurred at random (the real distribution has no longitude dependence). The lower the probability of the observations arising from a random distribution, the more likely is the presence of a longitudinal control.

[21] For post-noon South, we calculate the probabilities of the densest concentration of events in all continuous 180° regions. The probabilities are 0.16 for pre-equinox (11 of 17 events from 240° to 60°) and 0.15 for post-equinox (15 of 24 events from 330° to 150°). These probabilities are the lowest from any continuous 180° region and therefore the most favorable to show the presence of a longitudinal control. However, they are still too large to conclude a southern longitudinal control of the post-noon events.

[22] For the near-midnight distributions, the probabilities are 9.5×10^{-7} for pre-equinox North (20 of 20 events from 60° to 270°) and 6.1×10^{-5} for post-equinox South (20 of 22 events from 90° to 270°). These probabilities are extremely low and suggest that, contra *Chen and Hill* [2008], there is a longitudinal control in the injections, and further, that control varies with the Saturnian season. We note that the lack of post-equinox North longitude prevents us from knowing whether that seasonal variation is restricted to South.

4. Conclusions

[23] We performed an analysis of injection events in the Cassini RPWS data, from July 2004 through December 2011, which possess the characteristic emissions described by *Rymer et al.* [2009]. We have examined these events with respect to L shell, local time, and the newest SKR-derived

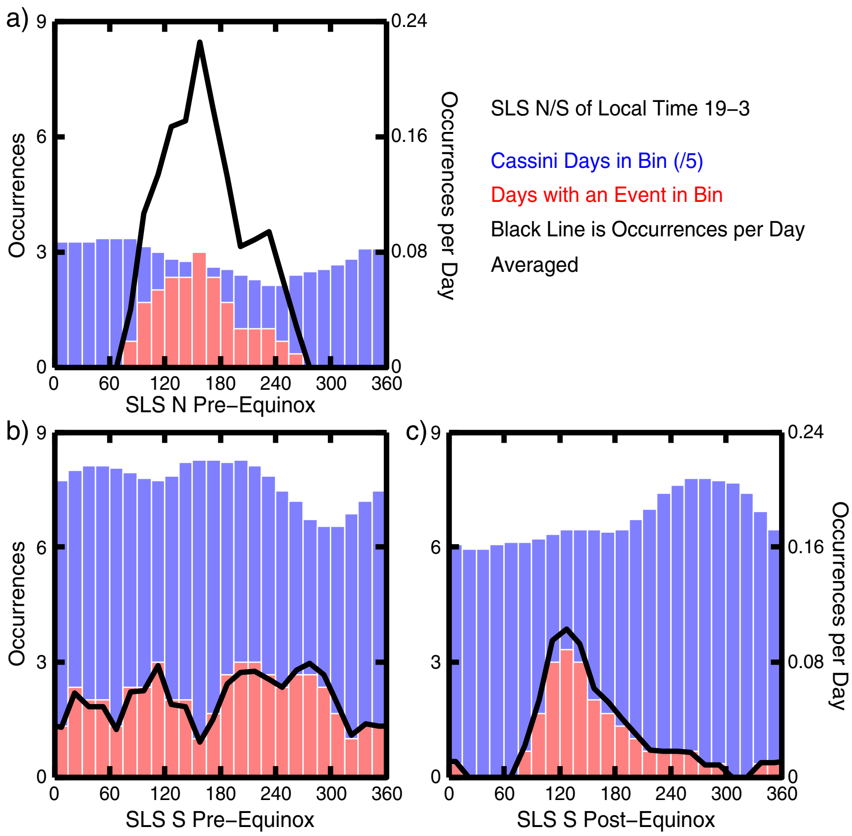

Figure 3. Pre-equinox and post-equinox longitude distributions of near-midnight injection events. The bin sizes are 15°. The days Cassini visited each bin are represented by the blue bars and are divided by five for visibility. The red bars represent the number of injection events observed in that bin. There are (a) 20 events in the SLS North pre-equinox, (b) 50 events in the SLS South pre-equinox, and (c) 22 events in the SLS South post-equinox histograms. The heights of the blue and red bars represent number of occurrences and the black lines represent occurrences per day. The missing blue bar in plot (a) is obscured by the red bar and has a value of 2.67.

longitude system (SLS 4) [*Gurnett et al.*, 2011] in order to search for spatial structure in their occurrence rate. To reduce observation biases, this study was restricted to low-inclination orbits when the spacecraft was inside an L shell of 12 and within 2 R_S of the equatorial plane.

[24] Our occurrence rate with respect to L shell largely agrees with the distribution published by *Chen and Hill* [2008]. In local time (Figure 2), however, we find that post noon (11–17 LT) and near midnight (19–3 LT) are preferred regions for injection event creation. This is substantially different from the clustering of plasma injections in the pre-noon quadrant (6–12 LT) in *Chen and Hill* [2008]. Since that study used a velocity profile for the ambient plasma, its back tracing to the source location may have underestimated the azimuthal speed of the flux tubes.

[25] In the older SLS 3 system, which is equivalent to SLS 4 South for its time period, *Chen and Hill* [2008] found no ordering in injection events from the first 26 Cassini orbits (pre-equinox) across all local times. Even though we studied different populations, we also find no ordering in SLS 4 South pre-equinox for all local times.

[26] We examined SLS 4 longitude ordering in the post-noon and near-midnight sectors, where *Radioti et al.* [2009] and *Mitchell et al.* [2009] observed separate phenomena related to large-scale injection events. For the post-noon sector's event distribution, we could not rule out a random longitudinal distribution in SLS South. This was true whether we treated all of the events together or separated them by time relative to the equinox.

[27] The near-midnight events show structure in North pre-equinox (Figure 3a) and South post-equinox (Figure 3c). The probabilities for these distributions to have occurred by chance are 9.5×10^{-7} and 6.1×10^{-5}, respectively. These probabilities are low enough to conclude that a probable longitudinal control is present in the creation of injection events and that this control varies with the Saturnian season for SLS South. The lack of post-equinox North longitudes prevents us from examining that occurrence distribution, but we might expect it to be unordered like the pre-equinox South distribution during that hemisphere's summer.

[28] These results suggest that the interchange instability is capable of communicating periodicities from the outer magnetosphere toward 6 R_S. The periodicities would originate near midnight and would vary with the Saturnian season. The hemispheric switch at equinox may imply that a change in the ionospheric conductivity is affecting the

interchange growth rate [*Southwood and Kivelson*, 1989] or that the change in the solar wind direction relative to the equatorial plane has effects on internal dynamics. For the conductivity suggestion to apply, there would need to be a low-conductivity anomaly in each hemisphere that only has an effect when that pole is dark.

Appendix A: Binning Process

[29] When multiple injection events are observed in a short time frame, they either were launched individually or were launched as a single event that broke up before passing the spacecraft [*Russell et al.*, 2005]. From the RPWS data alone, it is not possible to definitively state which one is the case for any given cluster of events. A goal of this study is to test for injection event ordering in local time and SLS (N and S) longitude. Those results could be skewed by cases where the events occur in clusters. We use a binning method that compensates for this effect. In both the one-dimensional (Figure 3) or two-dimensional (Figure 2) histograms, the counting is performed in bins and depends not upon the number of injections observed or the time that Cassini spent in a location, but rather just on the presence of any number of injections while Cassini was in that bin. The occurrence rate that we calculate (the black lines in Figures 2 and 3) is then the ratio of the number of passes through a bin with at least one event to the total number of passes through that bin. Therefore, this occurrence rate determines the regions that consistently create injection events.

[30] In the local time and L shell histograms, Cassini can only pass through a given bin once per orbit. In the SLS histograms, however, Cassini spends longer than one Saturnian day (as seen by the spacecraft) in the inner magnetosphere. In this case, the counts are allowed to increase each day. It is possible, then, that a single event would be double counted if it crossed over the spacecraft twice, but this is highly unlikely. The event would be much older than the ages that *Chen and Hill* [2008] calculated, and the spacecraft also moves away from the L shell of the first observation.

[31] After event sorting, the histograms were smoothed using a running average. The one-dimensional histogram averaging window was three bins wide. The two-dimensional running average was performed with a 3×3 box. The white region marks where Cassini made only one pass or where less than three bins would have contributed to the average and were excluded from both the averaging and the analysis. The one-dimensional histograms in Figure 2 were generated by summing the Cassini days and event counts along each column/row.

[32] One artifact of this binning method is that events are counted differently between different histograms. During the same orbit or Saturnian day, two events can fall into the same bin with one histogram but separate bins in another. As the catalogue of events grows, we expect that this effect would be minimal. However, this effect is visible in our data set, where we have a relatively small number of events. In Table 1, we observe ten North and eight South events that lie outside of our local time sectors even though every event with a North longitude has a South longitude. This is the only such artifact we have found in our analysis. It does not influence our study in a meaningful way, but we note its presence.

[33] **Acknowledgments.** We thank M. K. Dougherty for providing the magnetometer data used in this study. This research has been funded by NASA through contract 1415150 with the Jet Propulsion Laboratory.

References

André, N. et al. (2007), Magnetic signatures of plasma-depleted flux tubes in the Saturnian inner magnetosphere, *Geophys. Res. Lett.*, *34*, L14108, doi:10.1029/2007GL030374.

Burch, J. L., J. Goldstein, T. W. Hill, D. T. Young, F. J. Crary, A. J. Coates, N. André, W. S. Kurth, and E. C. Sittler Jr. (2005), Properties of local plasma injections in Saturn's magnetosphere, *Geophys. Res. Lett.*, *32*, L14S02, doi:10.1029/2005GL022611.

Chen, Y., and T. W. Hill (2008), Statistical analysis of injection/dispersion events in Saturn's inner magnetosphere, *J. Geophys. Res.*, *113*, A07215, doi:10.1029/2008JA013166.

Dougherty, M. K., et al. (2005), Cassini magnetometer observations during Saturn orbit insertion, *Science*, *307*, 1266–1270, doi:10.1126/science.1106098.

Gurnett, D. A., et al. (2004), The Cassini radio science investigation, *Space Sci. Rev.*, *114*, 395–463, doi:10.1007/s11214-004-1434-0.

Gurnett, D.A., et al. (2005), Radio and plasma wave observations at Saturn from Cassini's approach and first orbit, *Science*, *307*, 1255–1259, doi:10.1126/science.1105356.

Gurnett, D. A., A. Lecacheux, W. S. Kurth, A. M. Persoon, J. B. Groene, L. Lamy, P. Zarka, and J. F. Carbary (2009), Discovery of a north-south asymmetry in Saturn's radio rotation period, *Geophys. Res. Lett.*, *36*, L16102, doi:10.1029/2009GL039621.

Gurnett, D. A., J. B. Groene, T. F. Averkamp, W. S. Kurth, S.-Y. Ye, and G. Fischer (2011), The SLS4 longitude system based on a tracking filter analysis of the rotational modulation of Saturn kilometric radiation, in Planetary Radio Emissions VII, pp. 51–64, Austrian Acad. Sci., Vienna.

Hill, T. W. (1976), Interchange stability of a rapidly rotating magnetosphere, *Planet. Space Sci.*, *24*, 1151–1154, doi:10.1016/0032-0633(76)90152-5.

Hill, T. W., A. M. Rymer, J. L. Burch, E. J. Crary, D. T. Young, M. F. Thomsen, D. Delapp, N. Andre, A. J. Coates, and G. R. Lewis (2005), Evidence for rotationally driven plasma transport in Saturn's magnetosphere, *Geophys. Res. Lett.*, *32*, L14S10, doi:10.1029/2005GL022620.

Hospodarsky, G. B., T. F. Averkamp, W. S. Kurth, D. A. Gurnett, J. D. Menietti, O. Santolik, and M. K. Dougherty (2008), Observations of chorus at Saturn using the Cassini Radio and Plasma Wave Science instrument, *J. Geophys. Res.*, *113*, A12206, doi:10.1029/2008JA013237.

Krimigis, S. M., et al. (2005), Dynamics of Saturn's magnetosphere from MIMI during Cassini's orbital insertion, *Science*, *307*, 1270–1273, doi:10.1126/science.1105978.

Kurth, W. S., A. Lecacheux, T. F. Averkamp, J. B. Groene, and D. A. Gurnett (2007), A Saturnian longitude system based on a variable kilometric radiation period, *Geophys. Res. Lett.*, *34*, L02201, doi:10.1029/2006GL028336.

Kurth, W. S., T. F. Averkamp, D. A. Gurnett, J. B. Groene, and A. Lecacheux (2008), An update to a Saturnian longitude system based on kilometric radio emissions, *J. Geophys. Res.*, *113*, A05222, doi:10.1029/2007JA012861.

Leisner, J. S., C. T. Russell, K. K. Khurana, M. K. Dougherty, and N. André (2005), Warm flux tubes in the E-ring plasma torus: Initial Cassini magnetometer observations, *Geophys. Res. Lett.*, *32*, L14S08, doi:10.1029/2005GL022652.

Mauk, B. H., D. J. Williams, and R. W. McEntire (1997), Energy-time dispersed charged particle signatures of dynamic injections in Jupiter's inner magnetosphere, *Geophys. Res. Lett.*, *24*(23), 2949–2952, doi:10.1029/97GL03026.

Mauk, B. H., D. J. Williams, R. W. McEntire, K. K. Khurana, and J. G. Roederer (1999), Storm-like dynamics of Jupiter's inner and middle magnetosphere, *J. Geophys. Res.*, *104*(A10), 22,759–22,778, doi:10.1029/1999JA900097.

Mauk, B. H., et al. (2005), Energetic particle injections in Saturn's magnetosphere, *Geophys. Res. Lett.*, *32*, L14S05, doi:10.1029/2005GL022485.

Menietti, J. D., O. Santolik, A. M. Rymer, G. B. Hospodarsky, A. M. Persoon, D. A. Gurnett, A. J. Coates, and D. T. Young (2008), Analysis of plasma waves observed within local plasma injections seen in Saturn's magnetosphere, *J. Geophys. Res.*, *113*, A05213, doi:10.1029/2007JA012856.

Mitchell, D. G., et al. (2009), Recurrent energization in the midnight-to-dawn quadrant of Saturn's magnetosphere, and its relationship to auroral UV and radio emissions, *Planet. Space Sci.*, *57*, 1732–1742, doi:10.1016/j.pss.2009.04.002.

Müller, A. L., J. Saur, N. Krupp, E. Roussos, B. H. Mauk, A. M. Rymer, D. G. Mitchell, and S. M. Krimigis (2010), Azimuthal plasma flow in the Kronian magnetosphere, *J. Geophys. Res.*, *115*, A08203, doi:10.1029/2009JA015122.

Persoon, A. M., D. A. Gurnett, W. S. Kurth, G. B. Hospodarsky, J. B. Groene, P. Canu, and M. K. Dougherty (2005), Equatorial electron density measurements in Saturn's inner magnetosphere, *Geophys. Res. Lett.*, *32*, L23105, doi:10.1029/2005GL024294.

Radioti, A., D. Grodent, J.-C. Gérard, E. Roussos, C. Paranicas, B. Bonfond, D. G. Mitchell, N. Krupp, S. Krimigis, and J. T. Clarke (2009), Transient auroral features at Saturn: Signatures of energetic particle injections in the magnetosphere, *J. Geophys. Res.*, *114*, A03210, doi:10.1029/2008JA013632.

Russell, C. T., M. G. Kivelson, and K. K. Khurana (2005), Statistics of depleted flux tubes in the Jovian magnetosphere, *Planet. Space Sci.*, *53*, 937–943, doi:10.1016/j.pss.2005.04.007.

Rymer, A. M., et al. (2009), Cassini evidence for rapid interchange transport at Saturn, *Planet. Space Sci.*, *57*, 1779–1784, doi:10.1016/j.pss.2009.04.010.

Siscoe, G. L., and D. Summers (1981), Centrifugally driven diffusion of iogenic plasma, *J. Geophys. Res.*, *86*(A10), 8471–8479, doi:10.1029/JA086iA10p08471.

Southwood, D. J., and M. G. Kivelson (1989), Magnetospheric interchange motions, *J. Geophys. Res.*, *94*(A1), 299–308, doi:10.1029/JA094iA01p00299.

Tao, X., R. M. Thorne, R. B. Horne, S. Grimald, C. S. Arridge, G. B. Hospodarsky, D. A. Gurnett, A. J. Coates, and F. J. Crary (2010), Excitation of electron cyclotron harmonic waves in the inner Saturn magnetosphere within local plasma injections, *J. Geophys. Res.*, *115*, A12204, doi:10.1029/2010JA015598.

Wilson, R. J., R. L. Tokar, M. G. Henderson, T. W. Hill, M. F. Thomsen, and D. H. Pontius Jr. (2008), Cassini plasma spectrometer thermal ion measurements in Saturn's inner magnetosphere, *J. Geophys. Res.*, *113*, A12218, doi:10.1029/2008JA013486.

Young, D. T., et al. (2005), Composition and dynamics of plasma in Saturn's magnetosphere, *Science*, *307*, 1262–1266, doi:10.1126/science.1106151.